

Magnetic properties in the electron-doped bulk manganites $\text{Nd}_{1-x}\text{Ce}_x\text{MnO}_3$

Shixiong Zhang, Shun Tan, Wei Tong, and Yuheng Zhang*

Structure Research Laboratory, University of Science and Technology of China, Hefei 230026, People's Republic of China

(Received 23 March 2004; revised manuscript received 31 January 2005; published 21 July 2005)

In this paper, the magnetic properties in the electron-doped manganites $\text{Nd}_{1-x}\text{Ce}_x\text{MnO}_3$ ($x=0.04, 0.08, 0.10$) are reported. For $x=0.04$ sample, as the temperature increases, the magnetization (M) under zero field cooling (ZFC) changes from ferromagnetic (FM) to antiferromagnetic (AFM) and then back to FM again, and finally to paramagnetic (PM). The M - T curves under ZFC show that there are two peaks at about 15 K and 60 K, respectively and hence a valley between 15 K to 60 K. The M under field cooling (FC) of 0.024 T exhibits a large negative value at 5 K and achieves a positive maximum at 15 K, and then transforms to PM with the temperature increasing. With magnetic field increasing, for ZFC M - T , the valley changes from negative to positive, and disappears together with the peak at 60 K gradually. For FC M - T , the M at 5 K is changed from negative to positive, and the maximum M at 15 K shifts to lower temperature and disappears at 5 T. Combining with the M - H results, these phenomena can be explained by Néel's ferrimagnetic model, and the M - T curve under 0.024 T FC is well fitted by the molecular field theory. For $x=0.08$ and 0.10, as the temperature increases, the magnetization transforms from FM to PM gradually.

DOI: 10.1103/PhysRevB.72.014453

PACS number(s): 75.47.Lx, 75.50.Gg, 32.30.Dx

I. INTRODUCTION

The doped perovskite manganites $R_{1-x}A_x\text{MnO}_3$ (R =rare earth, A =other cation) have been widely investigated due to their interesting physics properties and their potential applications.¹⁻³ The parent compound RMnO_3 is a typical insulator, and the Mn^{3+} moments form an A -type antiferromagnetic structure due to the superexchange interaction between the Mn^{3+} ions.

Since the Mn ions in the electron doped manganites are the mixture of Mn^{2+} and Mn^{3+} , some authors suggested that the conductive mechanism in these systems should be the double exchange (DE) interaction which is correlated with the hopping of the e_g^2 electron between Mn^{2+} and Mn^{3+} .⁴⁻⁹ Moreover, they indicated that both Mn^{4+} and Mn^{2+} are non Jahn-Teller ions, whereas Mn^{3+} is a Jahn-Teller ion.^{5,7,10} However, Mitra *et al.*³ pointed out that there are 5 electrons in the $3d$ orbit of Mn^{2+} . So it is very possible that the additional (doped) electrons occupy the t_{2g} ↓subband rather than e_g ↑subband when the weak Hund's rule coupling $U_H < \Delta_{cf} + \Delta_{JT}$. In this case, they suggested that the general explanation of transport and magnetic properties of colossal MR manganites in terms of double exchange as the dominant mechanism needs a closer examination regardless of their high half-metallic transport character.

Although there remains contradictions on whether the interaction between Mn^{2+} and Mn^{3+} is double exchange, the insulator (I)-metal (M) transition accompanied with PM-FM transition was observed in electron-doped manganites $R_{0.7}\text{Ce}_{0.3}\text{MnO}_3$ (R =rare earth) as well as in the hole doped manganites.^{4-6,10} As we know, the parent compound NdMnO_3 is an A -type AFM insulator but it is still not know how the magnetic structure changes from the A -type AFM to FM ($T < T_c$) with the increase of doping level in the electronic doped systems.

In this paper, the magnetic properties of the low Ce-doped manganite $\text{Nd}_{1-x}\text{Ce}_x\text{MnO}_3$ ($x=0.04, 0.08, 0.10$) are studied

to investigate how the system evolves from the AFM state to the FM state. The temperature dependence of magnetization under zero field cooling (ZFC) for $\text{Nd}_{1-x}\text{Ce}_x\text{MnO}_3$ shows that upon warming, the magnetization (M) changes from ferromagnetic (FM) to antiferromagnetic (AFM) then back to FM again, and finally to paramagnetism (PM). The magnetization under field cooling (FC) of 0.024 T exhibits a large negative value, which can be explained by molecular field theory. The magnetization for $x=0.08, 0.10$ samples show that the system gradually exhibits weak FM characters at low temperatures.

II. EXPERIMENT

The polycrystalline samples of $\text{Nd}_{1-x}\text{Ce}_x\text{MnO}_3$ ($x=0.04, 0.08, 0.10$) compounds were prepared by conventional solid-state reaction methods. A stoichiometric mixture of Nd_2O_3 , CeO_2 , MnO_3 powders was heated at 1100 °C for 48 h with intermediate grindings. The final sintering process was carried out at 1400 °C for 24 h, and the samples were cooled with the furnace to room temperature. The structure and phase purity of samples were checked by powder x-ray diffraction (XRD) using Cu $K\alpha$ radiation at room temperature. Magnetization measurements were performed by using a Lake-Shore 9300 vibrating sample magnetometer (VSM).

Our x-ray-diffraction patterns show that all the samples are single phase with the structure of NdMnO_3 . The XRD patterns are shown in Fig. 1, and all the peaks can be indexed according to $Pbnm$ symmetry. We refined the crystal structures by GSAS program and show all the important factors, including the lattice parameters, the t factors, Mn-O bond lengths, Mn-O-Mn bond angles, and reliability factors R_p , in Table I. At the first glance, the bond length and angle have nothing to do with the doping content x . However, we notice that the radii of Nd^{3+} , Ce^{4+} , Mn^{3+} , Mn^{2+} are 127 pm, 114 pm, 64.5 pm, and 83 pm,¹¹ respectively. It indicates that the Nd(Ce)-O plane deflates while the Mn-O plane expands.

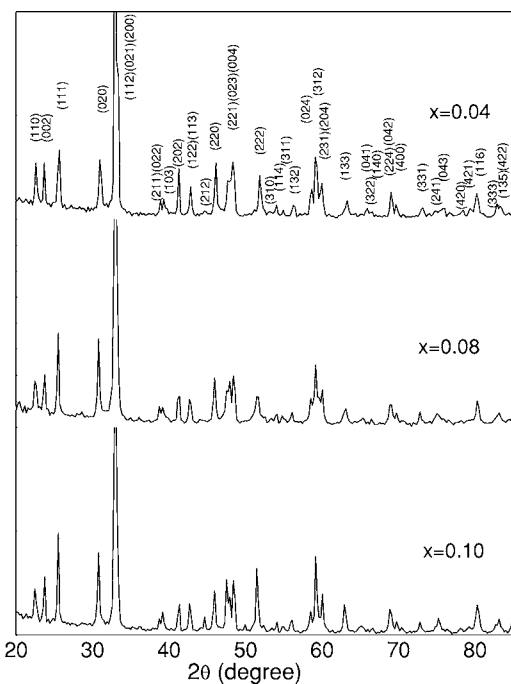


FIG. 1. Room temperature XRD spectra for $\text{Nd}_{0.90}\text{Ce}_{0.10}\text{MnO}_3$.

Therefore, there exists competition between the structure of *A*-site and *B*-site and thus the change of the bond constants is not monotonic. The little change of the lattice parameters and *t* factors should be attributed to the average effect.

III. RESULTS AND DISCUSSION

A. $x=0.04$

1. The change of magnetic state

In Fig. 2, we display the magnetization as a function of temperature (*M-T*) obtained under ZFC and FC with 0.024 T for $\text{Nd}_{0.96}\text{Ce}_{0.04}\text{MnO}_3$. The irreversibility between the ZFC and FC *M-T* curves can be seen clearly. Upon warming, the ZFC *M* drops rapidly at 15 K, crossing zero at 20 K, to a minimum negative value at $T=25$ K. After that, it increases slowly to a positive value and achieves a maximum one at 60 K, and then it decreases gradually as a PM behavior, forming a small peak at about $T=60$ K and a valley from 20 K to 60 K. However, the FC *M-T* curve shows a negative value at 5 K, then increases rapidly to a positive maximum, and finally decreases upon warming.

2. Coercivity

We also investigated the *M-H* relationship at some typical temperatures (as shown in the inset of Fig. 2). The hysteresis

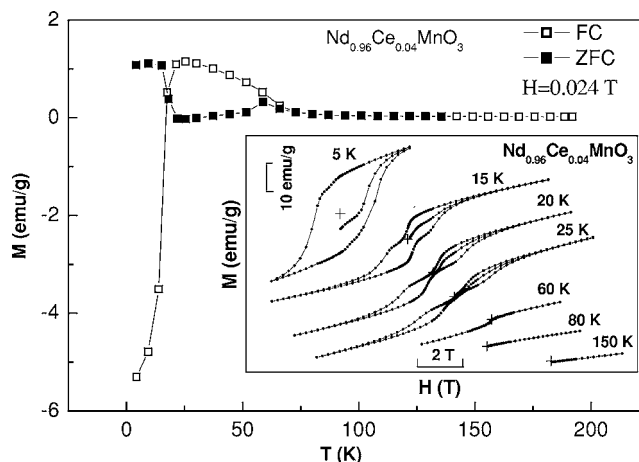


FIG. 2. ZFC and FC *M-T* curves for $\text{Nd}_{0.96}\text{Ce}_{0.04}\text{MnO}_3$ sample; the inset shows *M-H* curves at different temperatures.

loop, which is measured after cooling to 5 K under 0.024 T, displays a large coercivity about 1.2 T. The initial *M-H* curve shows that the magnetization linearly and slowly increases from a negative value to zero with the magnetic field enhances until 1.0 T, and then has an abrupt rise to the saturation. The hysteresis loop at 15 K has a coercivity around 0.5 T and it looks like a dumbbell which reveals the AFM behavior. In the initial *M-H* curve, the magnetization increases under low field, and then gradually tends to saturation. The shape of the 20 K-loop and 25 K-loop is similar to that of the 15 K-loop, while their coercivities are much smaller. For example, the coercivity (H_c) at 25 K is about zero. At 60 K where the little peak in ZFC curve locates, the *M-H* curve shows no hysteresis but it is nonlinear, indicating a FM behavior. At higher temperatures, the linear behavior is observed at 80 K, 150 K, which illustrates that the system has already been in the PM state.

3. Discussions on the ZFC and FC *M-T* results

All of the above magnetic results indicate that as the temperature increases, the magnetic structure under ZFC changes from FM to AFM, then back to FM again, and finally to PM. And *M* under FC changes from negative value to the positive maximum, then to PM. It is known that the Mn ions are the mixture of Mn^{2+} and Mn^{3+} in this system. With a slight Ce doping, the Mn^{2+} ions only replace the position of Mn^{3+} , but do not change the *A*-type AFM arrangement of the parent compound NdMnO_3 . The two planes, $\text{Mn}^{2+}/\text{Mn}^{3+}$ plane and pure $\text{Mn}^{3+}/\text{Mn}^{3+}$ plane, can be viewed as two sublattices. Both $\text{Mn}^{2+}/\text{Mn}^{3+}$ sublattice and pure $\text{Mn}^{3+}/\text{Mn}^{3+}$ sublattice are FM, but antiparallel with

TABLE I. The lattice parameters, *t* factors, Mn-O bond lengths, Mn-O-Mn bond angles, and reliability factors R_p for all compounds (O1 and O2 are two distinct oxygen sites in orthorhombic structure: the out-of-plane and the planar, respectively).

<i>x</i>	<i>a</i> (Å)	<i>b</i> (Å)	<i>c</i> (Å)	<i>t</i>	Mn-O1 (Å)	Mn-O2 (Å)	Mn-O1-Mn (°)	Mn-O2-Mn (°)	R_p
0.04	5.739(3)	7.474(9)	5.353(1)	0.8856	1.964(1)	1.376(6)/2.549(3)	144.0(8)	155.2(7)	0.1124
0.08	5.830(4)	7.533(3)	5.401(1)	0.8803	1.989(8)	1.361(0)/2.608(9)	142.5(2)	154.0(3)	0.1368
0.10	5.830(4)	7.537(5)	5.406(6)	0.8803	1.914(3)	1.997(1)/2.024(3)	159.2(7)	151.0(8)	0.1270

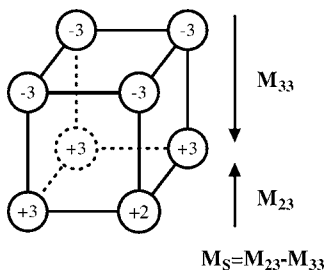


FIG. 3. Magnetic structure of $\text{Nd}_{0.96}\text{Ce}_{0.04}\text{MnO}_3$, the sign +, - indicate the directions of spin, M_S : the net magnetization, M_{33} : the magnetization of the pure $\text{Mn}^{3+}/\text{Mn}^{3+}$ sublattice, M_{23} : the magnetization of the $\text{Mn}^{2+}/\text{Mn}^{3+}$ sublattice.

each other (as shown in Fig. 3). For convenience, M_{33} represents magnetization of the pure $\text{Mn}^{3+}/\text{Mn}^{3+}$ sublattice, M_{23} represents magnetization of the $\text{Mn}^{2+}/\text{Mn}^{3+}$ sublattice and M_S represents the net magnetization of two sublattices. In Weiss's molecular field theory, M_{23} and M_{33} can be written as

$$M_{23} = N_{23}g_{23}S_{23}\mu_B B_{S_{23}}(y_{23}), \quad (1)$$

$$M_{33} = N_{33}g_{33}S_{33}\mu_B B_{S_{33}}(y_{33}), \quad (2)$$

$$y_{23} = g_{23}S_{23}\mu_B H_{23}/kT, \quad (3)$$

$$y_{33} = g_{33}S_{33}\mu_B H_{33}/kT, \quad (4)$$

where H_{23} and H_{33} are the total molecular fields acting on M_{23} and M_{33} , respectively, given by

$$H_{23} = H_0 + \gamma(-M_{33} + \beta M_{23}), \quad (5)$$

$$H_{33} = H_0 + \gamma(\alpha M_{33} - M_{23}), \quad (6)$$

$$M_S = M_{23} - M_{33}, \quad (7)$$

where α , β , and γ are the molecular-field coefficients. We did numerical calculation to the functions above and plotted the theoretical curve and the experimental data in Fig. 4. It is clear that our result, accords with this model very well. And

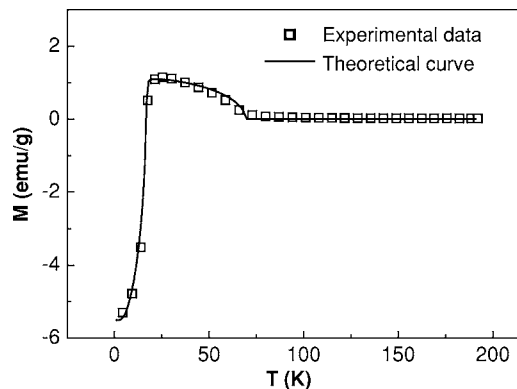


FIG. 4. The experimental and the theoretical M - T curves for $\text{Nd}_{0.96}\text{Ce}_{0.04}\text{MnO}_3$ under the FC process.

we also give the molecular-field coefficients as below: $\alpha = 3400$, $\beta = 2000$, $\gamma = 11000$.

The good fit of the theory with the experimental data should be attributed to two important things. First, the coercivity is very large at low temperature. For example, at 15 K where the FC magnetization decreases drastically, the coercivity H_S with 0.5 T is much larger than the applied field (0.024 T). In this case, it is impossible that the magnetic domains which are antiparallel with the applied field (H) flip to the H direction by force of the applied field. Secondly, we believe that M_{23} is parallel to the H direction while M_{33} is antiparallel to it. Thus formula (7) will be adaptable. When the system is under field cooling down to about 70 K which is below the magnetic ordering temperature, the DE interaction⁴ between Mn^{2+} and Mn^{3+} causes FM arrangement of $\text{Mn}^{2+}/\text{Mn}^{3+}$ planes. The coupling between the two sublattices ($\text{Mn}^{2+}/\text{Mn}^{3+}$ sublattice and pure $\text{Mn}^{3+}/\text{Mn}^{3+}$ sublattice) makes that the $\text{Mn}^{3+}/\text{Mn}^{3+}$ is in FM, but the arrangement between two sublattices is AFM. As a result, the net magnetization of the system is $M_S = M_{23} - M_{33}$. Keeping these two things in mind, we can understand the FC M - T curves clearly. M_{23} is larger than M_{33} above 17 K because M_{33} is induced by M_{23} , which results in the net magnetization $M_S > 0$ in the temperature range from 17 K to 70 K (see Fig. 4). Due to the $H_S = 0$ at $T > 25$ K, M_S is positive and prefers being parallel to the applied field. As the temperature decreases from 25 K, M_{33} increases much faster than M_{23} . The 17 K corresponding to $M_S = 0$ is the compensation point of the magnetization of the two sublattices. Below 17 K, M_{33} is much larger than M_{23} . Since the coercivity of this system is much larger than the applied measuring field as shown in the inset of Fig. 2 [for example, H_S (15 K) = 0.5 T \gg 0.024 T], the magnetic domains are locked in the original direction and M_{33} remains antiparallel to the applied field. Therefore the net magnetization should be a negative value.

During the ZFC process, the magnetic domains which are composed by two antiparallel sublattices are locked in random directions through the ordering temperature. When a measuring field of 0.024 T is applied at 5 K, the net magnetization $|M_S| = |M_{33} - M_{23}|$ is a small positive value because the magnetic moments which are parallel to the applied field are enhanced while those antiparalleling to the field are suppressed by the field. Upon warming, both M_{33} and M_{23} decrease, while M_{33} decreases more quickly than M_{23} . Since the measuring field is still smaller than the coercivity, it is hard for the domains to rotate. As a result, $|M_S|$ decreases as the temperature increases, but is still a negative value at 22 K. Due to the zero coercivity above 25 K, the domains can gradually rotate to the direction being parallel to the H -direction. Therefore M increases linearly upon warming to 50 K. When the temperature increases to higher than 50 K, M_{33} , instead of the domains, rotates to the direction being parallel to the applied field. Then both M_{23} and M_{33} are parallel to the applied field. Hence, a quick increase of M from 50 K to about 60 K and a FM behavior in the M - H curve at 60 K are observed (see Fig. 2). At higher tempera-

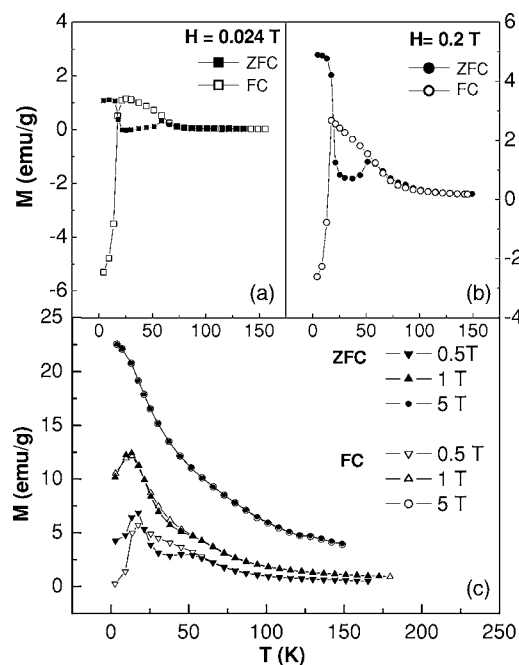


FIG. 5. M - T curves under different high applied fields for $\text{Nd}_{0.96}\text{Ce}_{0.04}\text{MnO}_3$ in both ZFC and FC processes: (a) $H=0.024$ T; (b) $H=0.2$ T; (c) $H=0.5$ T, 2 T, 5 T.

tures, the magnetic ordering in each plane is restrained and it is in the PM state, so M decreases and forms a peak at 60 K.

4. M - T relations under different magnetic field

To understand the novel magnetic behaviors of $\text{Nd}_{0.96}\text{Ce}_{0.04}\text{MnO}_3$ sample more deeply, we also performed the magnetization measurements in higher applied fields (0.2 T, 0.5 T, 1 T, 5 T). As for the ZFC curves, for $H=0.2$ T, the result in Fig. 5(b) is similar to that of $H=0.024$ T in Fig. 5(a). There appears a plateau at $T < 15$ K. When $T > 15$ K, the magnetization will drop with increasing temperature. Then a valley also appears in the range from about 15 K to 60 K, but the valley is positive. As $T > 60$ K, the system is in the paramagnetic state. For $H=0.5$ T, a peak appears at $T \approx 15$ K. A shallow valley is still shown and the minimum appears at $T \approx 40$ K [see Fig. 5(c)]. For $H=1$ T in Fig. 5(c), the same as the case of 0.5 T, there also exists a peak at $T \approx 10$ K, but there is no valley. The magnetization will decrease monotonically as $T > 10$ K. When the field increases up to 5 T, from Fig. 5(c) we can see that the peak disappears and no valley is exhibited. The magnetization will monotonically decrease with increasing temperature. As shown in Figs. 5(b) and 5(c), the shape of the FC curves under $H \leq 1$ T is similar to that of the 0.024 T, and the magnetization value increases with the enhancement of the applied field. Meanwhile, it can be seen that the difference between ZFC and FC M - T curves is faded with the field increasing. When $H=5$ T, the ZFC and FC M - T curves overlap entirely.

These M - T curves at various fields can be explained by combining with the M - H curves. In Fig. 6, we depict the initial M - H curves of the hysteresis loops at 5 K, 15 K and

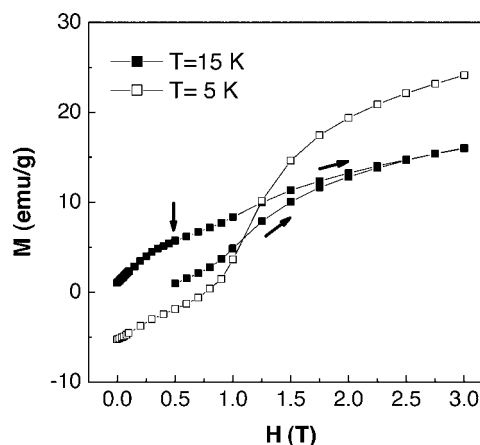


FIG. 6. The initial M - H curves at 5 K and 15 K and the hysteresis line at 15 K for $\text{Nd}_{0.96}\text{Ce}_{0.04}\text{MnO}_3$.

the hysteresis loop at 15 K in the first quadrant. As shown in Fig. 6, at 5 K, the initial linear M - H curve should be attributed to the rotation of domains with a net magnetization of $M_S = M_{23} - M_{33}$. And M_S of the domains have a tendency to be parallel to the field direction forced by the applied field. Whereas over the 1.0 T field, the M_{33} in the domain reverses to the direction of field, giving rise to the abrupt rise of magnetization. At 15 K, the initial M - H curve is different with that at 5 K, and it increases with the magnetic field. When $H > 0.5$ T, the M increases slowly as the field increases. Here, the 0.5 T is just equal to H_S (15 K). Therefore, the increase of initial magnetization in the M - H curve is primarily attributed to the collapse of the weak AFM coupling by the force of applied field. Obviously, at 15 K, the applied field of 0.024 T and 0.2 T is so small that it cannot change the AFM structure although it affects the value of the magnetization in both sublattices. When $T < 15$ K, in ZFC M - T curves, the magnetization value is almost unchanged with the increase of temperature, in the FC curves, all the magnetization values are negative below 15 K. With the increasing magnetic field to 0.5 T, the M_{33} flips to the field direction. The maximum M (e.g., $M_S = M_{23} + M_{33}$) in FC M - T curve is obtained. Above 15 K, similar to the M - T curve obtained under 0.024 T, the magnetization decreases upon warming. Therefore, both in the ZFC and the FC curves, there exhibits a sharp peak. When $H=1.0$ T, it is obvious that $M_S = M_{23} + M_{33}$ should occur below 15 K, and hence the sharp peak on M - T move to lower temperature. For $H=5$ T, this huge field forces almost all the magnetic moments to be parallel to the field direction, and thus the ZFC and FC M - T curves under 5 T display a monotonic drop upon warming.

There is a noteworthy thing in ZFC curves that the valley lifts up from negative ones to positive values when the applied field increases to 0.2 T. We noticed that the $\text{Mn}^{2+}/\text{Mn}^{3+}$ sublattice aligns along the field direction while the $\text{Mn}^{3+}/\text{Mn}^{3+}$ sublattice is antiparallel to it. The applied field reduces the magnetization of $\text{Mn}^{3+}/\text{Mn}^{3+}$ but enhances that of $\text{Mn}^{2+}/\text{Mn}^{3+}$, and so the net magnetization increases. When the field is higher, it destroys the AFM coupling between two sublattices and more and more magnetic moments turn to the H -direction. Therefore, the valley of the ZFC

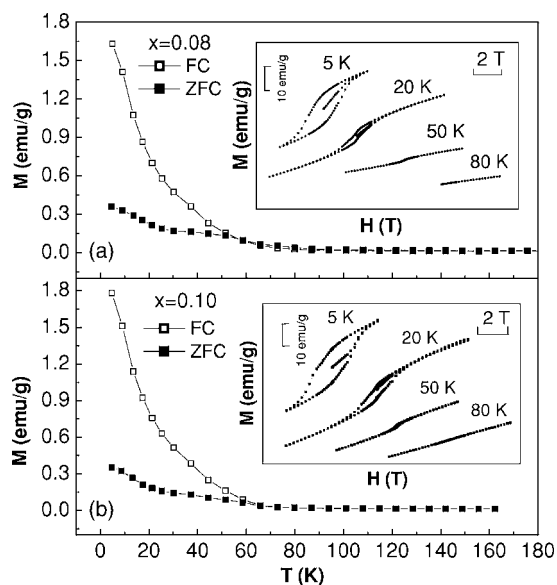


FIG. 7. The temperature dependence of magnetization for $\text{Nd}_{1-x}\text{Ce}_x\text{MnO}_3$ ($x=0.08, 0.10$) compounds under both (a) $x=0.08$ and (b) $x=0.10$; the insets show M - H curves at different temperatures for each sample.

M - T curve disappears when the applied field is large enough.

B. $x=0.08$ and 0.10

Figure 7 displays the temperature dependence of magnetization obtained under ZFC and FC with $H=0.024$ T for samples with $x=0.08, 0.1$. It is clear that the magnetic behaviors of these two samples are absolutely different from that of the $x=0.04$ sample. In the ZFC curves for both $x=0.08$ and 0.10 samples, the magnetization reduces as temperature increases from 5 K to 30 K, and in the range of 30–50 K there is a platform. While above 50 K, magnetization decreases slowly and the system enters the PM state. The magnetization in FC process rises promptly with the falling of the temperature from 60 K and when $T=5$ K, it is much greater than that in the ZFC process.

In the insets of Fig. 7, we depict the magnetic hysteresis loop at certain temperatures for $x=0.08, 0.10$. Clearly, the hysteresis loop at 5 K displays a FM character with large coercivity about 0.8 T. As the temperature increases, the coercivity H_S decreases quickly. The linear M - H curve at 80 K demonstrates a typical PM feature.

The difference magnetic behavior between $x=0.04$ and these two samples can be understood easily if one notices that the DE interaction between Mn^{2+} and Mn^{3+} enhances when the content of Mn^{2+} increases. The DE interaction becomes more stronger compared with the superexchange interaction between the Mn^{3+} ions in the pure $\text{Mn}^{3+}/\text{Mn}^{3+}$ plane. Therefore, the AFM structure formed by the anti-parallel arrangement of $\text{Mn}^{3+}/\text{Mn}^{3+}$ plane and $\text{Mn}^{2+}/\text{Mn}^{3+}$ plane is weakened and possible parallel arrangement is slowly formed. The parallel arrangement is very weak and in small zone, and thus the FM for the $x=0.08$ and 0.10 sample is weak and short range.

As we know, the magnetic state for NdMnO_3 is A -type AFM. From the above results and discussion, we can conclude that the magnetic property changes from AFM to ferrimagnetic and finally to weak ferromagnetic as Ce doping level increases from 0 to 0.10.

IV. CONCLUSION

In conclusion, we have studied the magnetic properties in the electron-doped manganites $\text{Nd}_{1-x}\text{Ce}_x\text{MnO}_3$ ($x=0.04, 0.08, 0.10$). For $x=0.04$ sample, as the temperature increases, M under ZFC changes from FM to AFM, then back to FM again, and finally to PM. The M - T curves under ZFC to 5 K and then measured in high fields show that there appear two peaks at about 15 K and 60 K, and a valley between 15 K to 60 K. The peak at 60 K and the valley disappears gradually when increasing the field to 1.0 T. The M under FC of 0.024 T exhibits a large negative value at 5 K, then transits to PM with the temperature increasing. The M - T curves under FC to 5 K and then measured in high field are similar to that in 0.024 T, but the M at 5 K changes from negative value to positive one gradually as the field increases. All the above phenomena can be explained by using Néel's ferrimagnetic model. The molecular field theory curve can fit the FC curve very well, and explain the large negative M in the FC M - T curve approvingly. For $x=0.08$ and 0.10 , as the temperature increases, the M transits from FM to PM gradually.

ACKNOWLEDGMENTS

The authors acknowledge Postdoctor Li Pi for helpful discussions. This work was supported by the Chinese National Science Foundation Grant No. 10334090 and the State Key Project of Fundamental Research, China (001CB610604).

*Electronic address: zhangyh@ustc.edu.cn

¹L. Balcells, R. Enrich, J. Mora, A. Calleja, J. Fontcuberta, and X. Obradors, *Appl. Phys. Lett.* **69**, 1486 (1996).

²C. Mitra, P. Raychaudhuri, G. Kobornik, K. Dorr, K.-H. Müller, L. Schultz, and R. Pinto, *Appl. Phys. Lett.* **79**, 2408 (2001).

³C. Mitra, P. Raychaudhuri, K. Dorr, K.-H. Müller, L. Schultz, P. M. Oppeneer, and S. Wirth, *Phys. Rev. Lett.* **90**, 017202 (2003).

⁴P. Mandal and S. Das, *Phys. Rev. B* **56**, 15073 (1997).

⁵C. Mitra, P. Raychaudhuri, J. John, S. K. Dhar, A. K. Nigam, and R. Pinto, *J. Appl. Phys.* **89**, 524 (2001).

⁶S. Roy and N. Ali, *J. Appl. Phys.* **89**, 7425 (2001).

⁷P. Raychaudhuri, C. Mitra, A. Paramakanti, R. Pinto, A. K. Nigam, and S. K. Dhar, *J. Phys.: Condens. Matter* **10**, L191 (1998).

- ⁸G. T. Tan, S. Dai, P. Duan, Y. L. Zhou, H. B. Lu, and Z. H. Chen, *Phys. Rev. B* **68**, 014426 (2003).
- ⁹P. Duan, G. T. Tan, S. Y. Dai, Y. L. Zhou, and Z. H. Chen, *J. Phys.: Condens. Matter* **15**, 4469 (2003).
- ¹⁰P. Raychaudhuri, S. Mukherjee, A. K. Nigam, J. John, U. D. Vaisnav, R. Pinto, and P. Mandal, *J. Appl. Phys.* **86**, 5718 (1999).
- ¹¹R. D. Shannon *et al.*, *Acta Crystallogr., Sect. A: Cryst. Phys., Diffr., Theor. Gen. Crystallogr.* **32**, 785 (1976); **32**, 751 (1976).